Research Article

Effect of pH on the stability of quartz in a multi-phase system of kaolinite, hydrous Al (hydr)oxide and quartz

Abdullah Musa Ali[1] · Eswaran Padmanabhan[2] · Abubakar Mijinyawa[1,3] · Mohammed Yerima Kwaya[1]

Abstract
The stability of quartz in a multi-phase system of kaolinite and Al (hydr)oxides and quartz has been addressed in quite a few studies. However, the impact of pH on these multi-mineral interactions has not been elucidated. Therefore, this study shows the different dissolution behaviour and surface morphology of quartz admixed with hydrous kaolinite and aluminium (hydr)oxides under variable pH conditions. This will enhance the predictability of silica behaviour in natural rock weathering and reservoir systems. Scanning electron microscopy characterization shows that kaolinite and Al (hydr) oxides exhibit high-quality coating of quartz surface at acidic and alkali pH by creating a surficial secondary layer that allows agglomeration of other minerals, while Fourier transform infrared analysis showed shifts in peak positions of Si–O quartz from 691 cm^{-1} and 692 cm^{-1} at pH 5 and 7 to 686 cm^{-1} at pH13, and broadening of characteristic hydroxide and siloxane peaks as well as the formation of new Si–O–Al bonds at pH 13, suggesting structural changes in hydrous aluminosilicates and Al hydroxides (broken bonds of Al–O–Si, Al–O–Al and Si–O–Si) and Al substitution for Si in tetrahedral sheets. The dissolved silica in quartz–kaolinite–Al (hydr)oxides interactions is relatively lower under alkali conditions compared to acidic pH. Quartz dissolution was highest at pH 7; signifying the interaction of quartz with Al (hydr)oxides and kaolinite is favourable for quartz dissolution at neutral pH range. The results indicate that quartz interaction with kaolinite and Al (hydr)oxides is dependent on pH. Quartz coating by kaolinite and Al (hydr)oxides is more effective under alkali pH conditions, given the low solubility of Al within this pH range.

Keywords Kaolinite · Al (hydr)oxides · FTIR characterization · Quartz dissolution

1 Introduction

Quartz is a fundamental material in reactions that affect porosity, permeability, capillarity buffering and sorption capacity of sandstones [11, 26, 49]. Recently, related studies have focused on quartz dissolution [4, 7, 20] because of the rising demand for rate information in compositionally intricate solutions derived from extreme conditions generated in systems such as nuclear waste disposal facilities and oil wells. Quartz grains are often associated with clays and aluminium (hydr)oxides in natural environments rather than as discrete separate forms. These multi-mineral interactions take place under different pH conditions, depending on the environment of deposition and diagenetic processes. Despite this association and ubiquitous coexistence of quartz, kaolinite and Al (hydr)oxides, majority of previous studies dealt with these minerals separately [27, 47]. Moreover, in the natural and man-made high pH environments, little is known regarding the effect of kaolinite and dissolved aluminium on the dissolution of quartz. It is thus pertinent to elucidate the multi-mineral interactions of quartz, kaolinite and hydrous Al (hydr)oxide across the pH spectrum to enhance the predictability of silica behaviour in natural rock weathering and reservoir

✉ Abdullah Musa Ali, alicorp07@gmail.com | [1]Department of Geology, Bayero University Kano, Kano, Nigeria. [2]Department of Geosciences, Universiti Teknologi PETRONAS, Seri Iskandar, Malaysia. [3]Centre for Geodesy and Geodynamics, National Space Research and Development Agency, Abuja, Nigeria.

SN Applied Sciences (2019) 1:388 | https://doi.org/10.1007/s42452-019-0398-3

Received: 11 November 2018 / Accepted: 23 March 2019 / Published online: 2 April 2019

systems. Deciphering these interactions will also help explain the dissolution behaviour and phase transition of silicates in alkali–acid leaching processes, which are crucial to microcrystalline purification and geochemical processes [5, 6, 8, 29, 48, 50, 51].

The stability of quartz in a multi-phase system of kaolinite, Al (hydr)oxides and quartz has been addressed in quite a few studies [2–4, 7, 14, 15]. Bickmore et al. [7] reported that dissolved Al ions at concentrations below the solubility of Al-(hydr)oxide significantly inhibit the dissolution of quartz. Since aluminium solubility increases with increasing pH in the basic region, its influence on dissolution rates will be important, whether the aluminium is derived from natural dissolution processes or by synthetic inclusion [7]. This study thus explores the role of pH in the interactions between quartz, kaolinite and Al-(hydr)oxide. Kaolinite was specifically included because the utilization of kaolinite is closely related to its reactivity and surface properties [19, 53, 54], which can be modified by interactions with quartz and Al-(hydr)oxides. The study also examines the coating of quartz grains by kaolinite and Al (hydr) oxides under different pH conditions. Scanning electron microscopy (SEM) and Fourier transform infrared (FTIR) spectroscopy were used because they effectively enable the characterization of mineral species [31, 38–42].

2 Materials and methods

2.1 Sample preparation and synthesis

A series of experiments were carried out to explore the combined effect of kaolinite and oxides/hydroxides of Al on quartz morphology and dissolution. White quartz sand used in the experiments was 99.8% SiO_2 according to energy-dispersive X-ray (EDX) analysis. The quartz crystals were crushed in a mortar grinder to increase the exposed surface area and then sieved to obtain > 50 µm mesh fraction. This pretreatment dissolved sharp edges, adhering fine particles and other surface contaminants without introducing metals or corrosive agents to the system that might affect subsequent dissolution rate measurements. The quartz grains were then ultrasonified in cold HNO_3 solution to remove any carbonate coatings and ferruginous contamination. The raw kaolinite used as precursor mineral was ground in an agate mortar, passed through a 125 µm sieve and then washed with hydrogen peroxide (H_2O_2) to remove organic residue. 0.1 g of kaolinite was added to Al_2O_3 dissolved in distilled water. Solutions were prepared using reagent grade NaOH, NaCl and Al_2O_3. In the first experiment, 0.1 g of kaolinite and 1 g of Aluminium oxides (Al_2O_3) were admixed with 2 g of quartz substrates in polyethylene bottles at variable pH of ≈ 5, 7, 13 to reflect different environment of deposition, given that kaolinite dissolves congruently at pH < 5 and > 11 [21]. It should be stated that the concentrations were selected arbitrarily, and the effect of the clay concentration was not considered. Buffer solutions of NaCl, KCl, NaOH and HCl were used to regulate the pH. The pH was adjusted with NaCl in drop-wise approach with constant stirring to attain a pH of 5 and 7. For pH of 13, 0.5 mol of NaOH was slowly added to the solution with the pH constantly measured. Solutions were immediately poured into the airtight polyethylene reaction vessels. The resultant slurry was briskly stirred using a magnetic stirrer for 15 min until a homogeneous mixture was obtained and left to rest for a period of 20 days.

Batch experiments were designed to measure quartz dissolution. Bottles were placed in a constant temperature bath of 60 °C. The amount of dissolved silica was measured after 20 days of ageing using molybdate spectrophotometry (HACH D2800). Upon removal from the bath, each bottle was unfastened and partly submerged in a beaker of the hot bath water for pH measurement at a temperature close to that of the bath. Solution pH was measured using a pH meter (EUTECH, Model: Cyberscan) with automatic temperature correction. pH measurements were made only to show that pH drift significantly during mineral interactions, which can affect their respective dissolutions.

2.2 Sample characterization

FTIR spectra were used for composition analysis and to identify disparity in chemical bonds. This method is based on the interaction between infrared (IR) electromagnetic radiation and the vibrational motion of atomic clusters. FTIR spectra were recorded at room temperature using a Shimadzu FTIR 8400S, which was linked to a desktop computer loaded with the software: Shimadzu labsolutions IR, to process the recorded spectra. Well-crystallized kaolinite was used in the experiment. Morphological characterizations of the samples were performed using scanning electron microscopy (SEM: Carl Zeiss Supra). The SEM–EDX analysis was carried out under low vacuum conditions to allow analysis of the uncoated samples by protecting against the build-up of static charge on the particle surfaces. Images of the surfaces were taken relative to the mounting, and by rotating and tilting the SEM stage to an angle between 45° and 55°. The bulk chemical results are based on the mapped data and exclude the direct influence of the carbon sticky pad.

3 Result

3.1 Quartz dissolution and pH measurement

Data on the experimental conditions for different admixtures of quartz (Q), kaolinite (K), aluminium (hydr)oxides

as well as measured silica dissolved from quartz are presented in Table 1. As observed, pH varies with the amount of dissolved silica in the system. At pH 5 and 13, the pH remained relatively steady after 20 days of ageing. In acidic conditions, OH^- ions dissolved from kaolinite ($Al_2SiO_5(OH)_4$) and aluminium (hydr)oxide ($Al(OH)_3$) (since both compounds are soluble at low pH) are released into the solution, causing the pH to increase. However, the pH dropped drastically at pH 7 to 4.75. The Q + K + Al system records values of 8.3 mg/L at pH 5, 9.2 mg/L at pH 7 and 1.7 mg/L at pH 13 (Table 1). The steep decline in pH from 7 to 4.75 and concomitantly high silica is characterized by distinctive grain bridging (Fig. 2b). Under neutral pH, the available OH^- ions are involved in the dissolution of quartz, and with continuous protonation, the pH declines over the duration of ageing. The agglomeration of the hydrous aluminosilicates over the quartz grains at pH 13 possibly limits the dissolution route of the alkaline solutions into the quartz grains, which accounts for the low silica in the system. Thus, the amount of dissolved silica in quartz–kaolinite interactions is relatively lower under alkali conditions compared to acidic pH. The dissolution of pure quartz grains was included in the experiment as control sample (Table 1). The amount of silica dissolved from pure quartz is significantly higher compared to the admixtures.

3.2 Morphological characterization using SEM

The dissolution process of kaolinite in HCl and NaOH solution was confirmed through changes in morphology from booklets to granulations and clay flakes as shown in Fig. 1. The dissolved kaolinite has no integral crystal structure and appears more like a transitional mineral phase, from booklets to granulations, clay flakes and platelets (Fig. 1). SEM micrographs were obtained for

Table 1 Experimental conditions for the admixture of Al (hydr)oxides (Al), kaolinite (K) and quartz (Q)

Sample	Time of ageing (days)	Ageing temperature (°C)	Initial pH	Final pH	Dissolved silica (mg/L)	Characteristic features
Q	20	60	12	11.8	35.6	Triangular etch pits; kink crystal faces
Q + K + Al	20	60	5.00	5.30	8.30	Grain coating and bridging
Q + K + Al	20	60	5.00	5.50	7.80	
Q + K + Al	20	60	5.00	5.40	8.10	
Q + K + Al	20	60	7.00	4.75	9.20	Grain coating and bridging
Q + K + Al	20	60	7.00	5	9.70	
Q + K + Al	20	60	7.00	5.20	9.60	
Q + K + Al	20	60	13.00	13.20	1.70	Shallow dissolution pits; higher grain coating
Q + K + Al	20	60	13.00	13.30	2.20	
Q + K + Al	20	60	13.00	13.10	1.65	

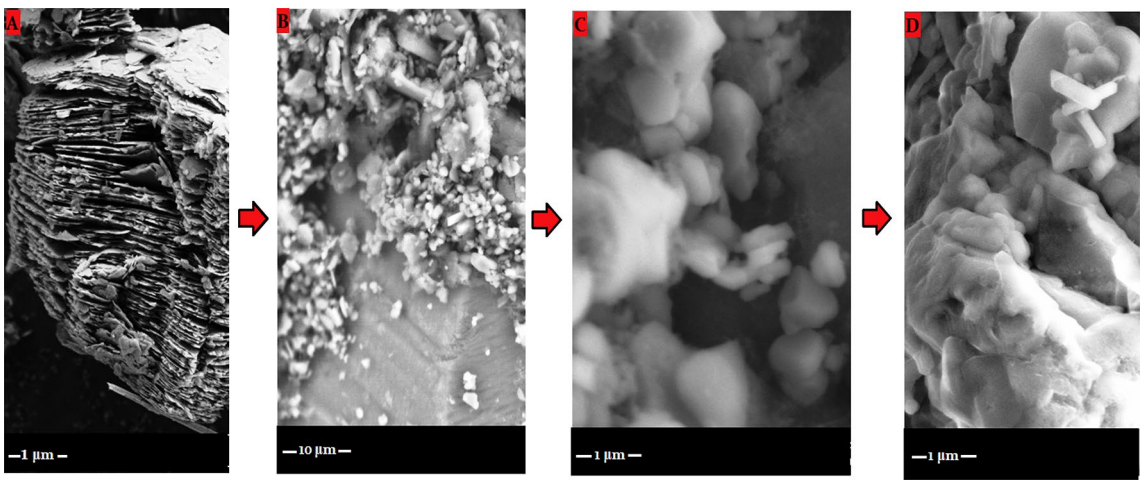

Fig. 1 SEM micrographs showing changes in the morphology of kaolinite from **a** booklets in low pH to **b** granulations near neutral pH, **c** clay flakes at neutral pH and **d** platelets at high pH

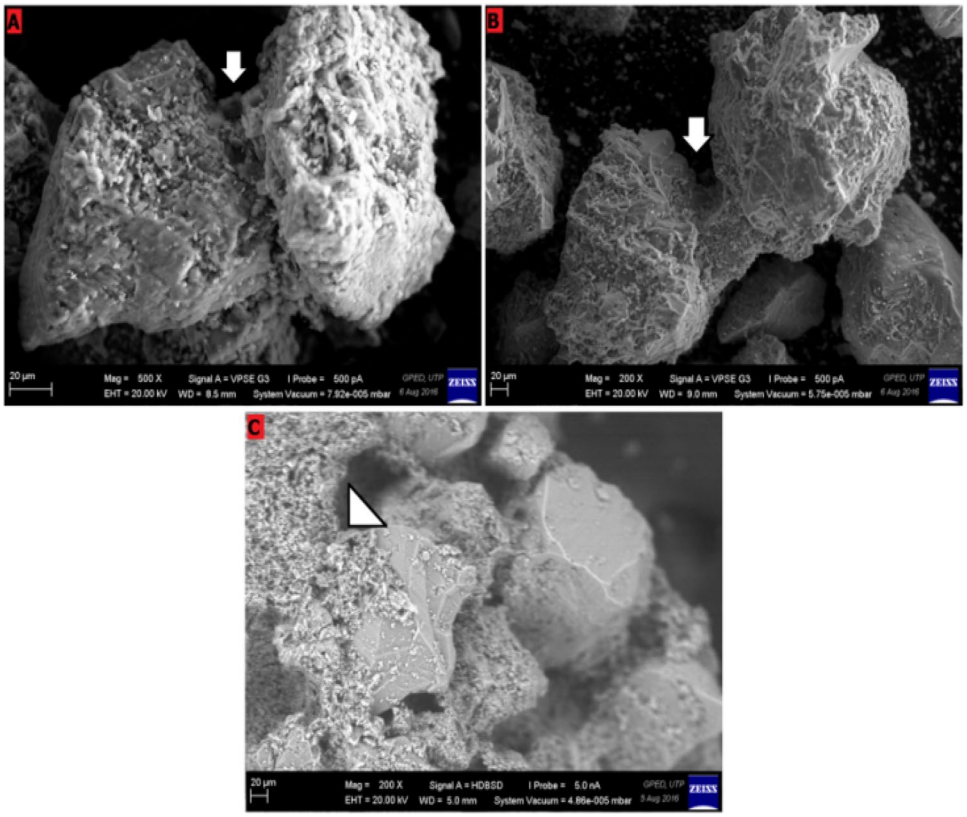

Fig. 2 SEM micrographs of Q + K + Al samples showing **a** slight grain bridging at pH 5, **b** quartz grain bridging by kaolinite and Al (hydr)oxides at pH 7, **c** agglomeration of the quartz grains by kaolinite and Al (hydr)oxides at pH 13

different admixtures of quartz (Q), kaolinite (K) and Al oxides aged in acidic, neutral and alkali pH media. The most discernible feature is the agglomerations or clustering of the quartz grains by kaolinite and hydrous Al oxide phase, as shown in Fig. 1. The bridging type, resulting from the adsorption of the kaolinite and hydrous Al hydroxides on quartz, is not dependent on the Al concentration. As explained in the sample preparation and experiment section, the concentration of quartz, kaolinite and aluminium oxides were maintained with only the pH being varied. The Al distribution is clearly different across pH, indicating that the bridging type is rather dependent on the dissolution and adsorption of Al on the quartz surface.

The SEM images of each of the analysed particle surfaces are presented in Fig. 2. The samples generally have a rounded morphology, although less smoothed, and a highly porous interior consisting of fine, irregular voids. Features characterizing the cluster of quartz, kaolinite and aluminium oxides (Q + K + Al) vary with pH (5, 7 and 13), as shown in Fig. 2. For acidic and neutral pH media, observed features include coating and bridging of quartz grains by kaolinite. At pH 5, the quartz grains are slightly cemented, as shown in Fig. 2a. Also observed is the deteriorating and flaking of the quartz surface (Fig. 2a) due to etching in the acid solution. The bridging of the quartz grains is more prominent and distinctive in samples aged in neutral solution (pH 7), as observed in Fig. 2b. In alkali solution, the quartz grains are characterized by shallow dissolution pits filled with kaolinite with relatively higher grain coating compared to the samples aged in acidic and neutral pH solutions (Fig. 2c). This suggests that quartz grains are better coated and agglomerated by aluminosilicates under alkali pH conditions. At alkali pH, dissolution and etched pits are present on the quartz surfaces in some places.

3.3 Micro-elemental distribution

The surface elemental composition of the samples was characterized using SEM–EDS to build a detailed picture of their surface structure and composition. The nature of compositional differences was investigated based on individual element maps and the results of targeted point analysis of different surface chemical phases. The elemental distribution maps of Si, O and Al for surfaces of Q + K + Al samples are shown in Figs. 3, 4 and 5. Al showed the most spatial heterogeneity in their distributions. The concentrations of Si and O are strongly localized across the quartz surface in the areas that appear darker on the SEM image. The Q + K + Al sample aged

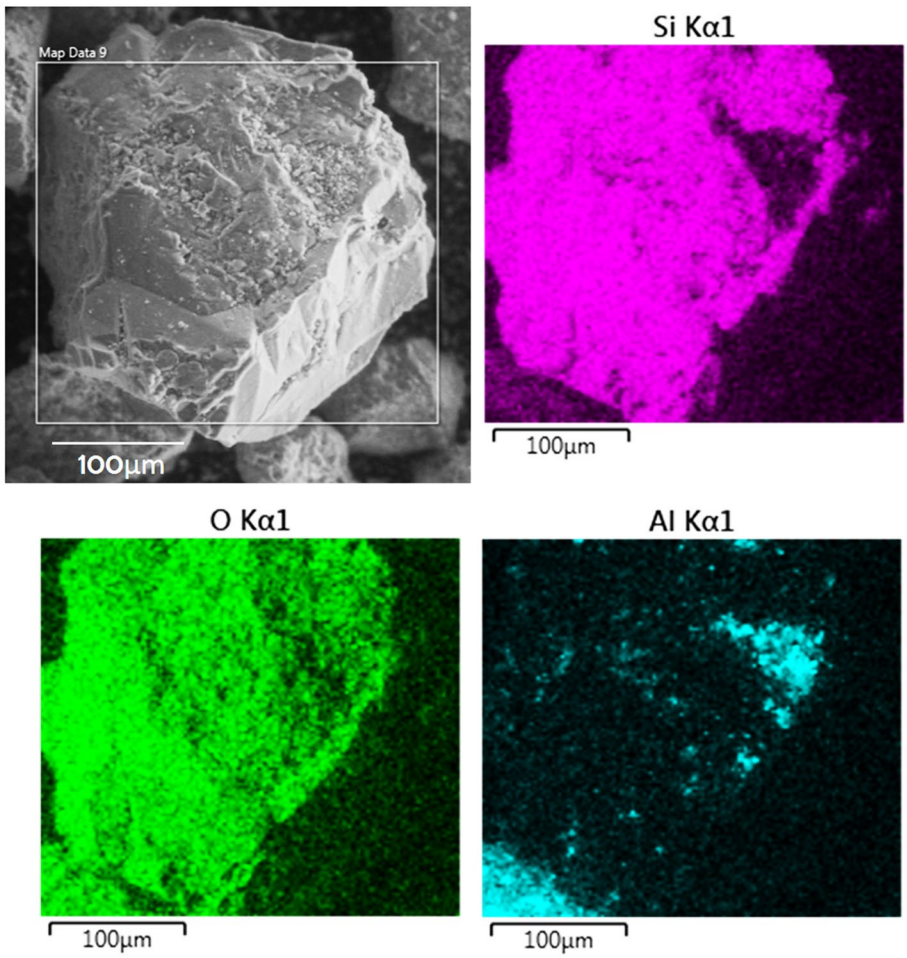

Fig. 3 EDX elemental mapping of quartz surface at pH 5, indicating Al accumulations in the fractures and crevices but absent on the smooth surface

at pH 5 showed that Al is aggregated at the fractured faces and crevices, while the smooth quartz surface remains bare, as indicated by the elemental distribution (Fig. 3), where Si and O are uniformly distributed, while Al accumulates in the surface defects. The isolated Al ions are embedded in the surface of the particle. The EDX mapping of the Q + K + Al sample aged at pH 7 (Fig. 4) shows that Al is relatively absent on the quartz surface, but rather forms the bulk composition of the bridge connecting the quartz grains. The EDX mapping of the Q + K + Al sample aged at pH 13 (Fig. 5) shows that Al leached from the kaolinite and Al (hydr)oxides are evenly distributed over the entire quartz surface, which suggest that quartz grains are better coated under alkali conditions.

Elemental mapping of the sample aged under alkali conditions (pH 13) shows that Si and O are uniformly distributed on the quartz surface. The wt% of the elements shows that Al is more dominant at pH 13 and less at pH 5, as shown in Fig. 6. This suggests that the Al element is more retained on the quartz surface under alkali conditions.

3.4 FTIR spectroscopic analysis

3.4.1 Low wave FTIR region

The characteristic IR peaks for the different samples were identified. In the low wave number region of the FTIR spectra (1400–400 cm^{-1}) shown in Fig. 7, the distinct absorption bands at 1030 cm^{-1} and 1006 cm^{-1} are ascribed to framework Si–O–Si stretching vibrations. The absorption bands at 936 cm^{-1} and 914 cm^{-1} represent the Al–OH bending vibrations. The band at 936 cm^{-1} is also attributed to the non-bonding inner-surface or surface (nanostructure) OH. The bands at 775 cm^{-1} and 697 cm^{-1} correspond to Al–OH or perpendicular surface ligands (translational OH). The absorption bands at 936 cm^{-1} representing the Al–OH bending are conspicuously absent at pH 13. In contrast, the absorption band at 864 cm^{-1} band for pH 13 (characteristic of the deformation vibration of

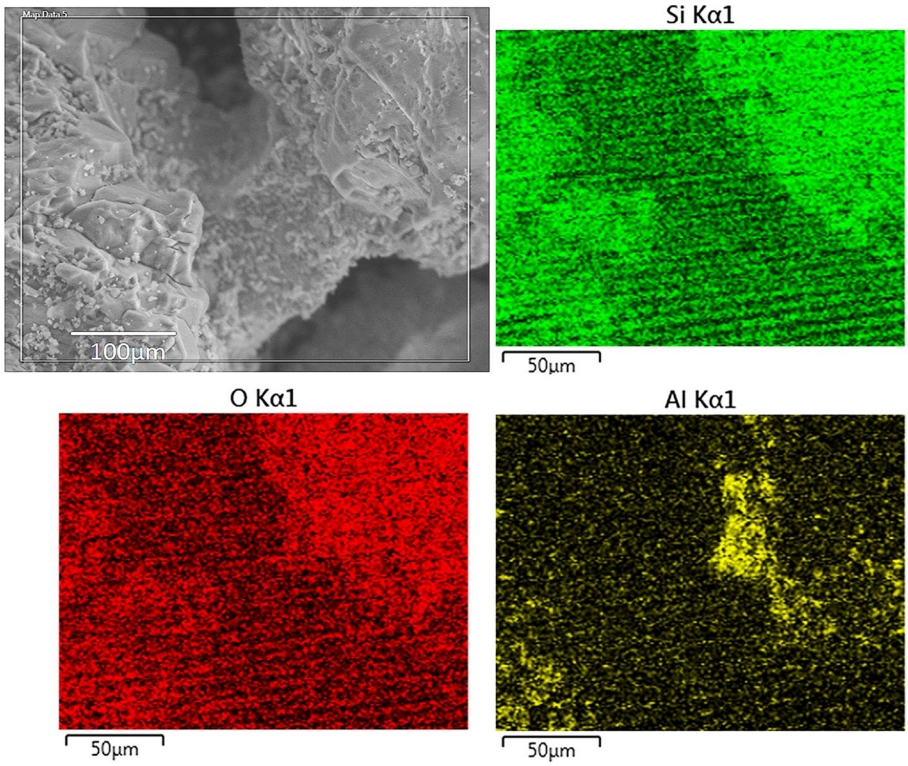

Fig. 4 EDX elemental mapping of the bridged quartz grains at pH 7, indicating the predominance of Al in the bridge connecting the quartz grains

bonded OH groups) is absent at pH 5 and 7. In addition, the Si–O–Al stretching peak shifted from 540 cm^{-1} at pH 13 to 545 cm^{-1} and 547 cm^{-1} at pH 5 and 7, respectively. Also observed is the band shifting of Si–O quartz peak from 691 cm^{-1} and 692 cm^{-1} at pH 5 and 7 to 686 cm^{-1} at pH 13. The siloxane (Si–O–Si) peak shifted from 657 cm^{-1} at pH 7 to 644 cm^{-1} at pH 13. This peak is absent at pH 7.

The broadening of the peak with increased pH indicates decreased crystallinity of the solid kaolinite phase [24]. The peaks at 1406 cm^{-1} and 1433 cm^{-1}, which are indicative of Al–O as Si cage (Si–O–Al), are only present in samples aged at pH 13. The presence of Si–O quartz characterized by the peak at 1084 cm^{-1} only for the sample aged at pH 7 suggests the poor kaolinite coating at neutral pH due to its non-dissolution at this pH.

3.4.2 Variations in hydroxide bonds

Given that structural order can influence morphology, it is important to examine the band parameters (bond variations) of inner OH deformation vibration and peak intensity as functions of the structural order/morphology. The inner hydroxyls of kaolinite–Al hydroxides are sited in the shared planes of octahedral sheet with the proton-end affixed in the ditrigonal hole [52]. The inner-surface hydroxyls are derived from the bonding of hydrogen atoms with oxygen atoms of neighbouring SiO_4 tetrahedral sheet. The basic unit cell of the hydroxyls holds 4 OH groups, indicating the presence of 4 OH stretching modes [34]. For the sample admixed at pH 5, three OH stretching vibration bands (3695, 3652 and 3620 cm^{-1}) emerged, while the characteristic hydroxyl peak at 3668 cm^{-1} is absent. Apart from the hydroxyl protons, there exists the proton of the physically adsorbed water in natural kaolinite. The peak at 3695 cm^{-1} can be assigned to the in-phase stretching mode of inner-surface OH groups or Al–OH stretching bond, while the peak at 3652 cm^{-1} can be ascribed to out-of-phase stretching modes of inner-surface OH groups. The peak at 3620 cm^{-1} denotes stretching of the inner OH group resulting from the bonding between a proton and an oxygen that is also coordinated to Al^{3+} in an octahedral site [18, 30]. These peaks become indistinct with increase in pH. At pH 7, the absorption peaks at 3652 cm^{-1} and 3668 cm^{-1} are absent, while the absorption band at 3695 cm^{-1} is the only prominent hydroxide band at pH 13 due to peak broadening and increased asymmetry caused by OH adsorption, as shown in Fig. 8.

4 Discussion

The results show that quartz interaction with kaolinite and Al (hydr)oxide is controlled by pH. SEM characterization showed variations in grain coating and quartz morphology for the different clusters. At acidic pH, relatively less Al is retained on the quartz surface, with

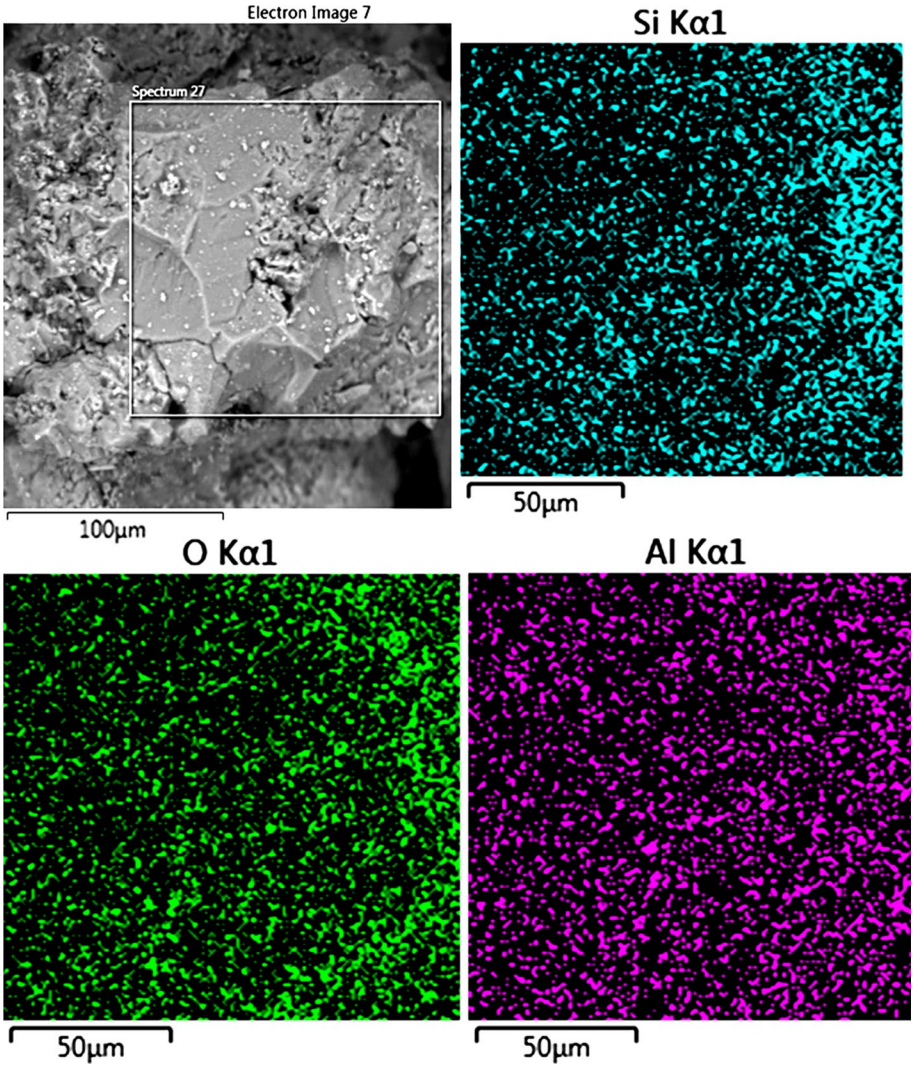

Fig. 5 EDX elemental mapping of quartz surface at pH 13, indicating the even distribution of Al on the quartz surface

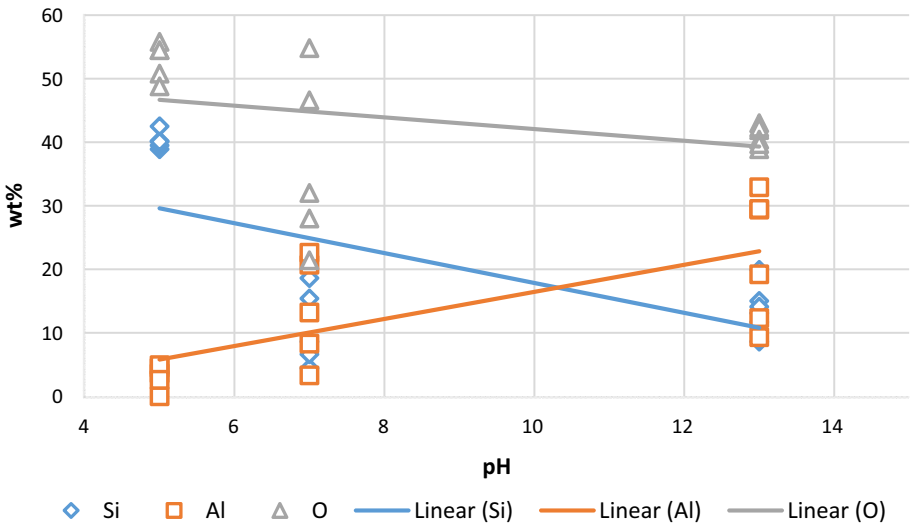

Fig. 6 Bulk chemical characterization of particle surfaces showing a plot of elemental weight (wt%) against pH for Si, Al, O

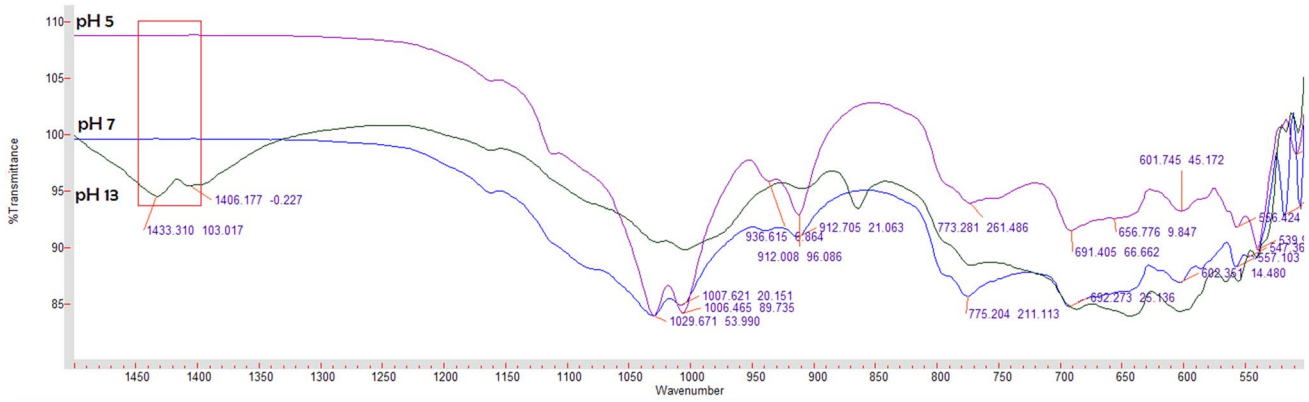

Fig. 7 Overlapping FTIR spectra of Q + K + Al synthesized at pH 5, 7 and 13 between 500 cm^{-1} and 1500 cm^{-1} showing the presence of Si–O–Al and inner Al–OH deformation for the sample synthesized at pH 13

morphological analysis indicating the outcome of etched quartz surfaces and low clay coating. Under neutral and alkali conditions, grain bridging and agglomerations were observed, respectively. This pH dependency of kaolinite dissolution has been attributed to the adsorption of H^+ and OH^- ions to aluminium and silicon reaction sites [9, 10, 12], in addition to the formation of positively, neutral and negatively charged aluminosilicate activated complexes at acid, near neutral and alkaline pH [1, 23]. In addition, the dissolved Al inhibits quartz dissolution in alkaline solutions; however, this study relates the inhibition of quartz dissolution to the adsorption of Al ions to the quartz surfaces, as shown in the SEM images and EDX analysis.

The structural changes in pure quartz with pH have been published in earlier papers [4, 35]. Quartz dissolution is generally higher at alkali pH, particularly hydroxides of monovalent ions such as K^+ and Na^+ because of their solvent properties (low hydrated cation radii and high hydrolysis constants). The dissolved quartz surface is typified by wide triangular etch pits and deep kink crystal faces. However, in this current paper, the dissolving effect is being inhibited by the presence of Al, insolubility of kaolinite at high pH and the occluding clay particles, which prevent the solution from reaching the bare quartz surface. This explains the relatively low amount of dissolved silica from quartz at alkali pH when admixed with kaolinite and Al (hydr)oxide.

The notion that sorbed Al inhibits quartz dissolution rates in alkaline solutions has substantial support in literature [17, 22, 44–46]. Adsorbed Al species have been revealed to qualitatively reduce silica dissolution rates in mildly alkaline solutions. In highly alkaline solutions, Al decreases silica dissolution to a larger extent, although most of the reviewed studies did not consider the saturation states of Al-(hydroxides). For example, Sasaki [37] observed that Al had a hindering effect on fused silica dissolution in 0.1 M NaOH at 95 °C (pH ~ 11.3), while Diallo et al. [16] showed that the dissolution rate of quartz was reduced by about a factor of 4 in the presence of Al in 0.1 N NaOH or KOH (pH ~ 11.8) at 70 °C. Labrid and Duquerroix [25] also observed that Al at 30 °C and pH 11.5 inhibited quartz sand dissolution rates. This study expands this theory by explaining possible interpretations of the phenomenon at different pH.

The different IR peak positions and intensities of the samples are attributed to the broken bonds of Al–O–Si, Al–O–Al and Si–O–Si and the Al substitution for Si in tetrahedral sheets [51]. The position of the hydroxyl and siloxane bonds depends on the outer chemical environment and on the morphology as a secondary structure [43]. The shifts and intensity disparity of the characteristic peaks can be attributed to changes or shifts in charges sited at the edges of kaolinite crystals [54], possibly resulting from the ageing process. The edge surface area is independent of the highly variable state of the interlayer space [54] but rather controlled by the broken fringes, particle diameter and shape. The surface broken bonds are the source of the pH-dependent charges, which become altered differently in variable pH media. For samples aged in alkali solution, bands characterizing OH groups at 3620 cm^{-1} and 3650 cm^{-1} disappeared completely, leaving behind a very low intensity peak at 3695 cm^{-1}. At the same time, the bands related to Si–O and Al–O vibrations in the range 1100–400 cm^{-1} were visibly broadened, indicating that the solid phase was gradually amorphous while the octahedral aluminium evolved into amorphous aluminosilicate structure [24]. These physical changes allow the absorption of Al ions onto the quartz grains, as indicated by the peak at 1400 cm^{-1}. Kaolinite dissolves in alkaline media, giving rise to silica $[SiO_2\ (OH)_2]^{2-}$ and

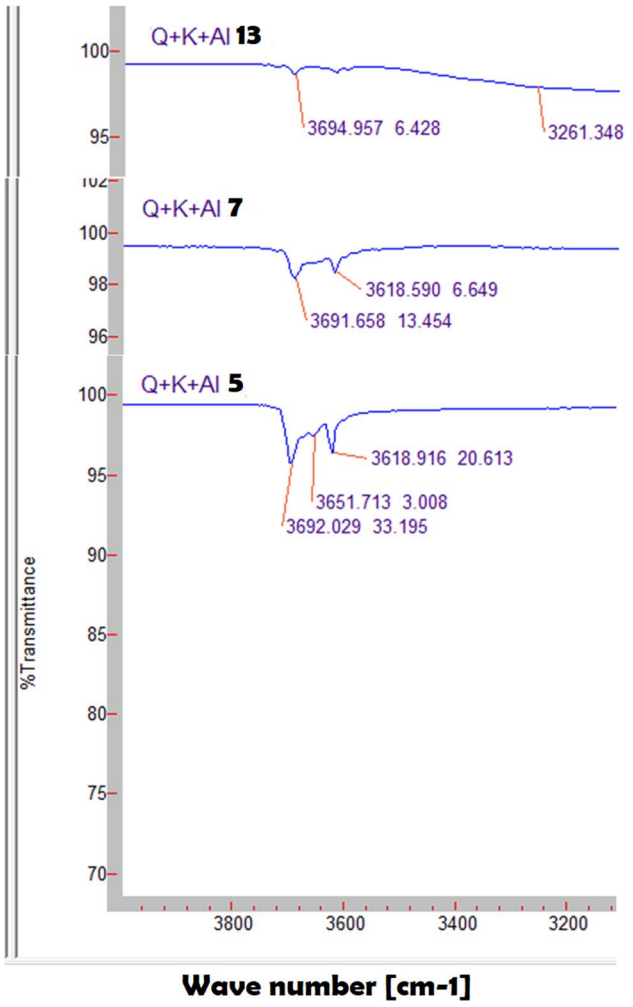

Fig. 8 Stacked FTIR spectra of Q + K + Al synthesized at pH 5, 7 and 13 between 3200 cm^{-1} and 4000 cm^{-1} showing the variations in hydroxide bonds at the different pH

$[SiO(OH)_3]^-$ as well as aluminium $[Al(OH)_4]^-$, which can inter-react to yield an aluminosilicate that precipitates in the form of a $Na_2O–Al_2O_3–SiO_2–H_2O$ gel or zeolite [28, 36, 48].

The changes in position of the surface OH groups can also be followed in the OH deformation range (950–850 cm^{-1}). The changes in the deformation coordinates of surface OH groups influence the position of the inner OH groups by changing the bond lengths/bond angles [54]. Since the inner OH groups are inert ones as compared to the surface OH groups, they can potentially be an indicator of the morphological variations that reflect changes in chemical environment, particularly pH. Although Zhang et al. [51] reported that the intensity changes of all kaolinite bands are mainly attributed to the increase of the structural defects in kaolinite layers, the competing Al ions are expected to impact on peak intensity. As shown in Fig. 9, the peak characterizing inner OH^- deformation for pH 13 suggests structural changes in Al–OH and Si–OH bonds. It also indicates that the inner-surface hydroxyls form the hydrogen bond with the oxygen of the adjacent SiO_4 tetrahedral sheet at this pH range.

As compared to the spectra of pristine kaolinite and quartz (Fig. 9), the intensity of absorbance peaks of kaolinite decreased considerably with interaction with quartz. The intensity of the %transmittance is highest at pH 5 and lowest at pH 7. This can be attributed to the fact that kaolinite dissolution generally decreases from pH 1 to 7, but increases from pH 8 to 12 [13]. The hydrous clay minerals and Al (hydr)oxides provide a relatively higher coating of quartz grains under alkali conditions. Spectral subtract of the Q + K + Al admixture aged at pH 13 from the spectra of pristine quartz, and kaolinite (Fig. 10) shows the formation of new bonds at 1400 and 864 cm^{-1}, which are characteristic of Si–O–Al and inner OH/Al–OH deformation, respectively.

Therefore, it can be inferred that the dissolution of quartz in natural and engineered systems will not only be affected by pH, but also influenced by its interaction with hydrous oxides and clay minerals. Similar atomic proportions of Al and Si in several areas within the interior regions of quartz coatings are supportive evidence for the bonding of kaolinite and quartz [32, 33]. To effectively predict the transport and reactivity of quartz in aquatic environments, the aggregation mechanisms between quartz and hydrous oxides and clay minerals and quartz should be taken into consideration.

5 Conclusion

The dissolution of quartz in a multi-phase system of quartz, hydrous oxides and clay minerals is controlled by pH. The results showed that Al oxides creates a surficial secondary phase that allows agglomeration of other minerals as well as produce derivative surface defects that mask the quartz morphology. Quartz grains are better coated and agglomerated by aluminosilicates under neutral and alkali pH conditions. The competing interactions of Al (hydr)oxides and hydrous kaolinite are indicated by the presence of Si–O–Al bonds and the broadening of quartz siloxane bonds, particularly under alkali conditions, which suggests that structural deformation is more active at high pH.

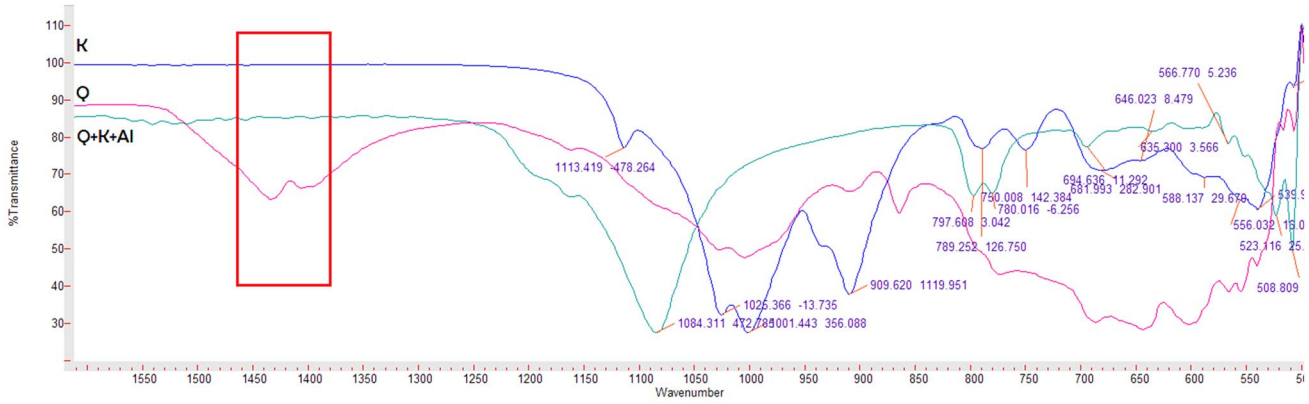

Fig. 9 Overlapping FTIR spectra of quartz, kaolinite and admixture of quartz, kaolinites and aluminosilicates aged at pH 13 between 500 cm^{-1} and 1500 cm^{-1} showing the presence of Si–O–Al and inner Al–OH deformation, and the absence of surface OH for the sample synthesized at pH 13

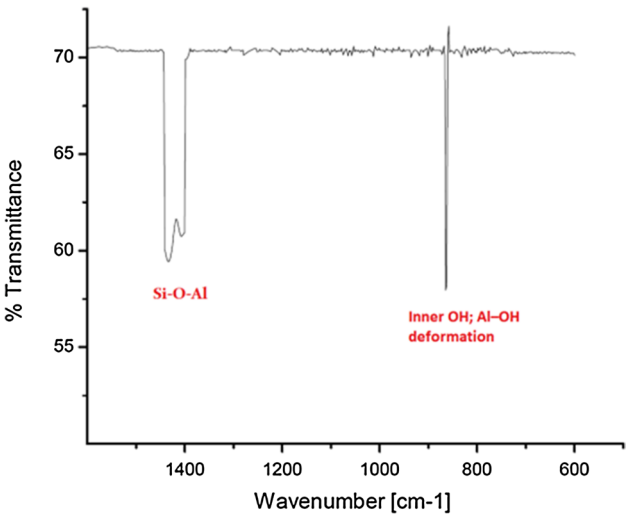

Fig. 10 FTIR spectral subtract of Q + K+Al from the spectra of pristine quartz and kaolinite

Funding The study was supported by the graduate assistantship scheme provided by the Universiti Teknologi PETRONAS. No part of the manuscript has been published or under consideration in other journals.

Compliance with ethical standards

Conflict of interest The authors declare that they have no conflict of interest.

References

1. Aagaard P, Hegelson HC (1982) Thermodynamic and kinetic constraints on reaction rates among minerals and aqueous solutions-I. Theoretical considerations. Am J Sci 282:237–285
2. Ali A, Padmanabhan E (2013) Quartz surface morphology of tertiary rocks from North East Sarawak, Malaysia: implications for paleo-depositional environment and reservoir rock quality predictions. Pet Explor Dev 41:6
3. Ali AM, Padmanabhan E (2017) The impact of pH and temperature on gibbsite reactivity with quartz. Int J Petrochem Res 1(1):40–45
4. Ali AM, Padmanabhan E, Baoiumy H (2017) Characterization of alkali induced quartz dissolution rates and morphologies. Arab J Sci Technol 42(6):2501–2513
5. Arias M, Barral MT, Diaz-Fierros F (1995) Effects of iron and aluminum oxides on the colloidal and surface properties of kaolin. Clays Clay Miner 43:406–416
6. Arias M, Barral MT, Diaz-Fierros F (1997) Comparison of functions for evaluating the effect of Fe and A1 oxides on the particle size distribution of kaolin and quartz. Clay Miner 32:3–11
7. Bickmore BR, Nagy KL, Gray AK, Brinkerhoff AR (2006) The effect of $Al(OH)_4$ on the dissolution rate of quartz. Geochim Cosmochim Acta 70:290–305
8. Bish D (1989) Rietveld refinement of non-hydrogen atomic positions in kaolinite. Clays Clay Miner 37(4):289–296
9. Blum AE, Yund RA, Lasaga AC (1990) The effect of dislocation density on the dissolution rate of quartz. Geochim Cosmochim Acta 54:283–297
10. Brady PV, Walther JV (1989) Control on silicate dissolution rates in neutral and basic pH solutions at 25 °C. Geochim Cosmochim Acta 53:2823–2830
11. Brantley SL, Kubicki JD, White AF (2008) Kinetics of water–rock interactions. Springer, New York
12. Carroll-Webb SA, Walther JV (1988) A surface complex reaction model for the pH-dependence of corundum and Kaolinite dissolution rates. Geochim Cosmochim Acta 52:2609–2623
13. Carroll-Webb SA, Walther JV (1990) Kaolinite dissolution at 25 °C, 60 °C and 80 °C. Am J Sci 290:797–810
14. Coston JA, Fuller CC, Davis JA (1995) Pb^{2+} and Zn^{2+} adsorption by a natural aluminum- and iron-bearing surface coating on an aquifer sand. Geochim Cosmochim Acta 59:3535–3547
15. Davis JA, Coston JA, Kent DB, Fuller CC (1998) Application of the surface complexation concept to complex mineral assemblages. Env Sci Technol 32:2820–2828
16. Diallo MS, Jenkins-Smith NL, Bunge AL (1987) Dissolution rates for quartz, aluminum bearing minerals, and their mixtures in sodium and potassium hydroxide, SPE paper 16276. In:

International symposium on oilfield chemistry, San Antonio, Texas, Feb. 4–6, pp 359–368
17. Dove PM (1995) Kinetic and thermodynamic controls on silica reactivity in weathering environments. In: White AF, Brantley SL (eds) Chemical weathering rates of silicate minerals, vol 31. Mineralogical Society of America, Short Course, Chantilly, pp 236–290
18. Farmer VC (1998) Differing effects of particle size and shape in the infrared and Raman spectra of kaolinite. Clay Miner 33:601–604
19. Huang G, Guo H, Zhao J, Liu Y, Xing B (2016) Effect of co-existing kaolinite and goethite on the aggregation of graphene oxide in the aquatic environment. Water Res 102:313–320
20. Hoch AR, Linklater CM, Noy DJ, Rodwell WR (2004) Modelling the interaction of hyperalkaline fluids with simplified rock mineral assemblages. Appl Geochem 19:1431–1451
21. Huertas FJ, Chou L, Wollast R (1999) Mechanism of kaolinite dissolution at room temperature and pressure part II: kinetic study. Geochim Cosmochim Acta 63:3261–3275
22. Iler RK (1955) The colloid chemistry of silica and silicates, 1st edn. Cornell University Press, Ithaca, p 324
23. Knauss KG, Wolery TJ (1988) The dissolution kinetics of quartz as a function of pH and time at 70 °C. Geochim Cosmochim Acta 52(1):43–53
24. Krol M, Mozgawa W, Jastrzebski W, Barczyk K (2012) Application of IR spectra in the studies of zeolites from D4R and D6R structural groups. Microporous Mesoporous Mater 156:181–188
25. Labrid J, Duquerroix JP (1991) Thermodynamic and kinetic aspects of the dissolution of quartz–kaolinite mixtures by alkalis. Revue de L'Institut Francais du Pétrole 46:41–59
26. Lasaga AC, Luttge A (2001) Variation of crystal dissolution rate based on a dissolution stepwave model. Science 291:2400–2404
27. Li H, Feng Q, Ou L, Long S, Cui M, Weng X (2013) Study on washability of microcrystal graphite using float–sink tests. Int J Min Sci Technol 23(6):855–861
28. Liu Y, Naidu R (2014) Hidden values in bauxite residue (red mud): recovery of metals. Waste Manag 34(12):2662–2673
29. Liu Q, Li X, Cheng H (2016) Insight into the self-adaptive deformation of kaolinite layers into nanoscrolls. Appl Clay Sci 124–125:175–182
30. Madejova J, Komadel P (2001) Baseline studies of the clay minerals society source clays: infrared method. Clays Clay Miner 49:410–432
31. Murad E (2010) Mössbauer spectroscopy of clays, soils and their mineral constituents. Clay Miner 45:413–430
32. Padmanabhan E, Mermut AR (1996) Sub-microscopic structure of Fe-coatings on quartz grains in tropical environments. Clays Clay Miner 44(6):801–810
33. Padmanabhan E, Kessler F (2008) Fabric variability within layered Fe-oxide deposits in Mid-Late Miocene sedimentary formations, NW Borneo: impact on facies architectural interpretations. Bull Geol Soc Malays 54(1):165–169
34. Prost R, Dameme A, Huard E, Driard J, Leydecker JP (1989) Infrared study of structural OH in kaolinite, dickite, nacrite, and poorly crystalline kaolinite at 5 to 600 K. Clays Clay Miner 37(5):464–468
35. Rimstidt JD (2015) Rate equations for sodium catalyzed quartz dissolution. Geochim Cosmochim Acta 167:195–204
36. Samal S, Ray AK, Bandopadhyay A (2013) Proposal for resources, utilization and processes of red mud in India—a review. Int J Miner Process 118:43–55
37. Sasaki B (1962) The corrosive action of aqueous solutions of several electrolytes on the silicic solid surfaces. Bull Chem Res Inst Non-Aqueous Solut Tohoku Univ 2:113–129
38. Schwertmann U, Taylor RM (1977) Iron oxides. In: Dixon JB, Weed SB (eds) Minerals in soil environments. Soil Science Society of America, Madison, pp 145–180
39. Schwertmann U, Murad E (1977) Effect of pH on the formation of goethite and hematite from ferrihydrite. Clays Clay Miner 31(4):277–284
40. Schwertmann U, Taylor RM (1989) Iron oxides. In: Dixon JB, Weed SB (eds) Minerals in soil environments, 2nd edn. Soil Science Society of America, Madison, pp 379–438
41. Schwertmann U, Cornell RM (1991) Iron oxides in the laboratory. VCH, Weinheim, p 137
42. Schwertmann U, Fitzpatrick RW (1992) Iron minerals in surface environments. In: Skinner HCW, Fitzpatrick RW (eds) Biomineralization processes of iron and manganese: modern and ancient environments, vol 21. Catena Supplement. Catena Verlag, Reiskirchen, pp 1–6
43. Táborosi A, Kurdi R, Szilágyi RK (2014) The positions of inner hydroxide groups and aluminium ions in exfoliated kaolinite as indicators for external chemical environment. Phys Chem Chem Phys 16:25830–25839
44. Van Bennekom AJ, Buma AGJ, Nolting RF (1991) Dissolved aluminum in the Weddell–Scotia confluence and effect of Al on the dissolution kinetics of biogenic silica. Mar Chem 35:423–434
45. Van Cappellen P, Qiu LQ (1997) Biogenic silica dissolution in sediments of the Southern Ocean. 1. Solubility. Deep Sea Res II 44:1109–1128
46. Van Cappellen P, Qiu LQ (1997) Biogenic silica dissolution in sediments of the Southern Ocean. 2. Kinetics. Deep Sea Res II 44:1129–1149
47. Van Ranst E, Padmanabhan E, Vandenberghe RE, De Grave E, Mees F (2016) Yellowing of a red south African Kandiudult studied by means of Mössbauer spectroscopy. Soil Sci 181:2
48. Wang H, Feng Q, Liu K (2016) The dissolution behavior and mechanism of kaolinite in alkali–acid leaching process. Appl Clay Sci 132–133:273–280
49. White AF, Bullen TD, Schulz M, Blum AE, Huntington TG, Peters NE (2001) Differential rates of feldspar weathering in granitic regoliths. Geochim Cosmochim Acta 65:847–869
50. Yang L, Steefel CI (2008) Kaolinite dissolution and precipitation kinetics at 22 °C and pH 4. Geochim Cosmochim Acta 72(1):99–116
51. Zhang M, Xu N, Peng Y (2015) The entrainment of kaolinite particles in copper and gold flotation using fresh water and sea water. Powder Technol 286:431–437
52. Zhu X, Zhu Z, Lei X, Yan C (2016) Defects in structure as the sources of the surface charges of kaolinite. Appl Clay Sci 124–125:127–136
53. Zsirka B, Horváth E, Makó É, Kurdi R, Kristóf J (2015) Preparation and characterization of kaolinite nanostructures: reaction pathways, morphology and structural order. Clay Miner 50:329–340
54. Zsirka B, Horváth E, Jarvas Z, Dallos A, Makó É, Kristóf J (2016) Structural and energetical characterization of exfoliated kaolinite surfaces. Appl Clay Sci 124–125:54–61